Int J Adv Manuf Technol (2012) 59:1211–1225
DOI 10.1007/s00170-011-3569-y

ORIGINAL ARTICLE

A new insertion strategy for a peg in an unfixed hole of the piston rod assembly

Jianhua Su · Hong Qiao · Chuankai Liu · Zhicai Ou

Received: 17 April 2011 / Accepted: 3 August 2011 / Published online: 26 August 2011

Abstract Sensorless manipulation strategies have been successfully used in the precision robotic assembly. Most previous work in this area has concentrated on inserting a peg into a fixed hole. However, in some cases, e.g., the assembly of piston–peg–rod of the automotive engine, due to the motion of piston, the position of the hole in piston is hard to be fully constrained. The purpose of this paper is to give a novel sensorless manipulation strategy for the high-precision assembly of a peg into an unfixed hole. Firstly, a decomposition method of the high-dimensional configuration space of the peg hole is analyzed. Subsequently, the robotic manipulations are proposed in the two low-dimensional spaces decomposed from the high-dimensional configuration space. Then, the attractive regions formed in the two sub-spaces are constructed, thus, the position and orientation uncertainties of the peg hole can be eliminated by the attractive regions and the robotic manipulations. Finally, a typical industry application, fitting a peg into an unfixed piston rod hole of the automotive engine, is used to validate the presented strategy.

Keywords Robotic assembly system · Sensorless strategy · Peg–piston–rod assembly

1 Introduction

Automated assembly system with a custom robot has grown increasing applications in manufacturing over the years. High-precision assembly, such as the tight-tolerance peg-in-hole insertion, is difficult to be accomplished by the position adjustment of the robotic system. Figure 1 demonstrates an example of high-precision insertion requirement in the automotive engine assembly line, where a peg should be inserted through the hole of piston and the hole of the small end of the rod. The peg, the piston, and the rod, which are used to push against the crankshaft, and convert the up and down motion of the piston to the rotary motion of the crankshaft, are the key workpieces of an automotive engine. The assembly operations for the three parts are very important but difficult, as: (a) the radius of the peg is about 27.9980–27.9925 mm, while the hole in the piston is 28.0000 mm with a tolerance of about 2–7.5 μm; (b) the motion of the round piston is hard to be fully prevented by the fixture, i.e., the piston hole is unfixed. In many situations, the robotic assembly is realized with a low-cost Remote Center Compliance (RCC) or by the guidance of a force sensor. However, the RCC device has no durability since it is made from rubber, and the force sensor is expensive and not so reliable. Therefore, a robotic peg-in-hole assembly system without force sensors or flexible wrists has an advantage in terms of durability, expense, and reliability.

In our previous work [1], the method of inserting a peg in a fixed hole had been discussed based on attractive region formed in three-dimensional configuration space. In this study, a strategy to achieve the high-precision task of inserting a peg in an unfixed hole is explored based on the attractive region formed in high-dimensional configuration space. Meanwhile, a robotic assembly prototype is built to validate the proposed strategy.

1.1 Related works

The objective of the robotic peg-hole assembly is to achieve high-precision insertion from an unknown initial peg-hole

J. Su (✉) · H. Qiao · C. Liu · Z. Ou
Institute of Automation, Chinese Academy of Sciences,
Room 705, Automation Building, No.95,
Zhongguancun EastRoad,
Beijing 100190, People's Republic of China
e-mail: jianhua.su@ia.ac.cn

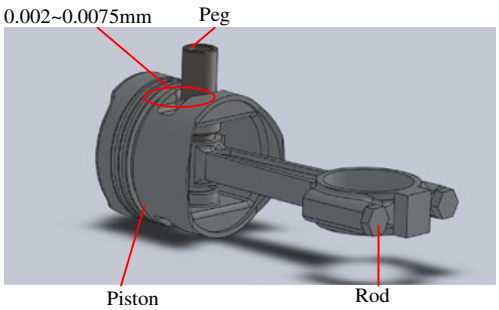

Fig. 1 The piston, piston peg, and connecting rod

configuration to a geometrical goal under some constraints. In the last decades, various robotic insertion strategies with force sensors or flexible wrists have been proposed. There are three primary methods in the previous strategies in this area.

1.1.1 Robotic assembly with force sensor

The utilization of force sensor in robotic assembly has been widely studied since the 1970s. The studies of Inoue [2] and Whitney [3] have been widely recognized as important examples in motion planning. Many other works have applied the assembly methods with a table force sensor or a wrist force sensor. Loiano et al. [4] proposed a strategy for inserting a peg into a piston hole based on the force sensor, where the state of contacts and the direction and magnitude of the inserting forces were predicted by the force sensor feedback. Schutter et al. [5] described an application of robotic assembly operation with active force feedback involving fragile and medium-sized workpieces. In their work, the interaction forces were used to modify or even generate the desired trajectory of the robot. Katz and Wyk [6] presented a search strategy for the peg-hole automated pre-assembly engagement. In their research, a position controlled X, Y-table was used to move the assembly surface in a prespecified search pattern, and a force/torque sensor feedback was used to detect an engagement configuration, terminating the search process. Yao and Cheng [7] derived the geometrical compatibility condition for the insertion motion where mating force/moment was free of overshooting, and the non-cylinder pairs mating were achieved by the aid of force sensors. Zhang et al. [8] modeled the peg-in-hole process as a discrete event system, where the assembly states were recognized with the force information. Tangjitsitcharoen et al. [9] used the torque sensor to control the position of the shaft during the assembly by setting the limit of torque to stop the motor driver of machine. Shirinzadeh et al. [10] presented a robotic-based height adjustment method for the assembly of a cylindrical pairs. In their paper, the peg-in-hole strategy was established by decreasing the contact forces between the manipulator and the fixture.

1.1.2 Robotic assembly with flexible wrists

Manufacturers cannot afford the initial setup and maintenance cost of force sensors. They find it practical to develop and implement a low-cost robotic system for the peg-hole insertion task. Thus, the RCC, which incorporates compliant motion for error correction during the assembly, has been developed to assist the peg-in-hole insertion. The utilization of the flexible wrists and the design principles were analyzed by Whitney [11] and Simunovic [12]. In recent years, over 100 various devices used in robotic assembly have been developed, such as the dynamic RCC established by Asada [13], the scanning assembly device designed by Ivanov [14], the Variable Remote Center Compliance developed by Lee [15]. The RCC devices are low cost and reliable for the round peg-in-hole insertions, and have successful industrial applications. But, the RCC method has some problems as follows: (a) it is no longer useful when there are hundreds of different contact states between the mating parts caused by the position uncertainty of the peg on the gripper [16]; (b) there is also no durability of the RCC device that is made from rubber material [17]. Therefore, for the case of the peg-in-piston-hole, where the peg and hole are hard to be fixed with high precision on the gripper or fixture, it is difficult to exert the effect of RCC method.

1.1.3 Robotic assembly without force sensors or flexible wrists

This approach makes use of constraints of the environment instead of additional devices to achieve high-precision operation. Caine et al. [18] initiated research on the planar peg-hole insertion operation by analyzing the insertion process from any unknown initial peg-hole configuration to the side-surface contact state without sensor. Matsuno [17] focused on the problem of inserting a long peg into a tandem shallow hole which is shaped uniquely. They used searched trajectory generation to acquire correct peg posture without feedback. Chen et al. [19] discussed the insertion of an accumulator into a hole in the valve body of an automatic transmission system. They applied the soft servo strategy to achieve the tight-tolerance assembly with the compliance of the robot and the environment. Qiao [1] presented the strategies of sensorless motion planning for the peg hole, and proved the validity of the strategies by the robots operations. Balkcom et al. [20] created sensorless plans that guaranteed a workpiece was correctly inserted into a fixture.

The previous works mainly discussed the problem that the peg could get two degrees of freedom on position translation as the hole is held firmly by the fixture. To the best of our knowledge, there is little work to explore the

case that the hole is not constrained in some degrees of freedom during the insertion process, which is also very significant in industry, such as the peg-in-piston assembly process in the automotive production.

1.2 The purpose of this paper

One difficulty in sensorless peg-hole insertion is how to achieve exactness, i.e., how to make sure that the planned path is exactly compliant to the desired contact state, especially when the configuration space of such a contact state is hard to describe analytically due to high dimensionality [21]. It is a challenge to insert a peg into a hole if it is hard to holding the motion on the hole, since the motion planning for the peg-in-hole task needs to be performed in a high dimensional configuration space.

Based on our previous work on the attractive region, the objective of this paper is to propose a new sensorless insertion strategy in the high-dimensional configuration space, and design a robotic system for the assembly of peg–piston–rod of the automotive engine. Our analysis is based on visible strategic behaviors by decomposing the high-dimensional configuration space into two low-dimensional configuration spaces. Then, the robotic inserting force can be determined in the sub-configuration spaces. And the motion of peg should be guaranteed to comply with the desired contacts. The main works of this paper include:

1. A robotic system, including a six DOF industry robot, a control computer, a fixture to hold the workpieces, and a camera to identify the target and guide the grasps, is established to assembly a peg, a piston, and a rod together.
2. The dynamic process of clamping the rod to the desired stable state, where the hole of rod is aligned to the hole of piston, is discussed. The relationship between the stable state of the rod and minimum of the attractive region is also analyzed, where the position uncertainty of the rod should be eliminated.
3. A peg-in-hole insertion strategy is designed based on the decomposition of the configuration space. The decomposition method makes the assembly be visible in the low-dimensional configuration space and guarantees the planned path compliance with the desired contact state.

The rest of this paper is arranged as follows: Section 2 presents the robotic assembly cell designed in the laboratory. In Section 3, the dynamic process of fixing the rod is investigated based on the attractive region formed in the configuration space of the rod fixture system. In Section 4, the insertion strategy based on the decomposition of configuration space of peg-hole system is presented. Finally, the whole assembly process is described with a real experiment to show the efficiency of the design strategy and the prototype.

2 Description of the robotic assembly system

The flexible robotic assembly system consists of a six DOF industrial robot, a fixture for holding workpieces, a CCD camera, and a control computer. The structure of the system is shown in Fig. 2.

As shown in the Fig. 2, three subsystems, i.e., the vision system, the robot and the fixture, are controlled by the computer. The application programs, such as the motion planning, image processing, are written with Microsoft Visual C++ software on the computer. In order to transfer the target position to the robot, an ActiveX module, named Fanuc robot I/F, supplies a channel to send the pose information to robot.

Each part of the assembly system is described as follows:

2.1 Robot

The robot chosen for the assembly application is M6i-B, which is a six-axis articulated robot for a variety of industrial applications. A pneumatic parallel-jaw gripper, SMC MHL-16D, is mounted on the robot to manipulate the peg, piston, and rod. The repeatability of M6i-B is ±0.08 mm, so that the high-precision requirement (inserting the peg into the hole with a tolerance about 2–7.5 μm) is difficult to be accomplished by the position adjustment of the custom industrial robot.

2.2 Image processing unit

The image processing unit consists of a Unikon color CCD camera for image acquisition, and a DS-4002MD image acquisition interface card of Hikvision Company. The camera has 704×576 pixels and 30 images per second. The function of the DS-4002MD is to convert the analog video signal into digital audio and store it in the image memory for computer processing. This interface card with PCI interface has 32Kbps–2Mbps image transmission speed. The camera mounted on the end of the robot is acted as an “eye” of the robot and provides the object pose information. Therefore, a target object with arbitrary pose should be identified from a set of parts on the conveyor.

2.3 Workpiece holding fixture

A workpiece holding fixture is designed to assist the manipulations of the robot. The operations of the fixture, including clamping the piston and rod, transmitting the end of the rod into the cavity of the piston, are controlled by an AT89S52 microprocessor. The synchronous network communication system between the computer and the microprocessor of the fixture consists of a RS485 converter to

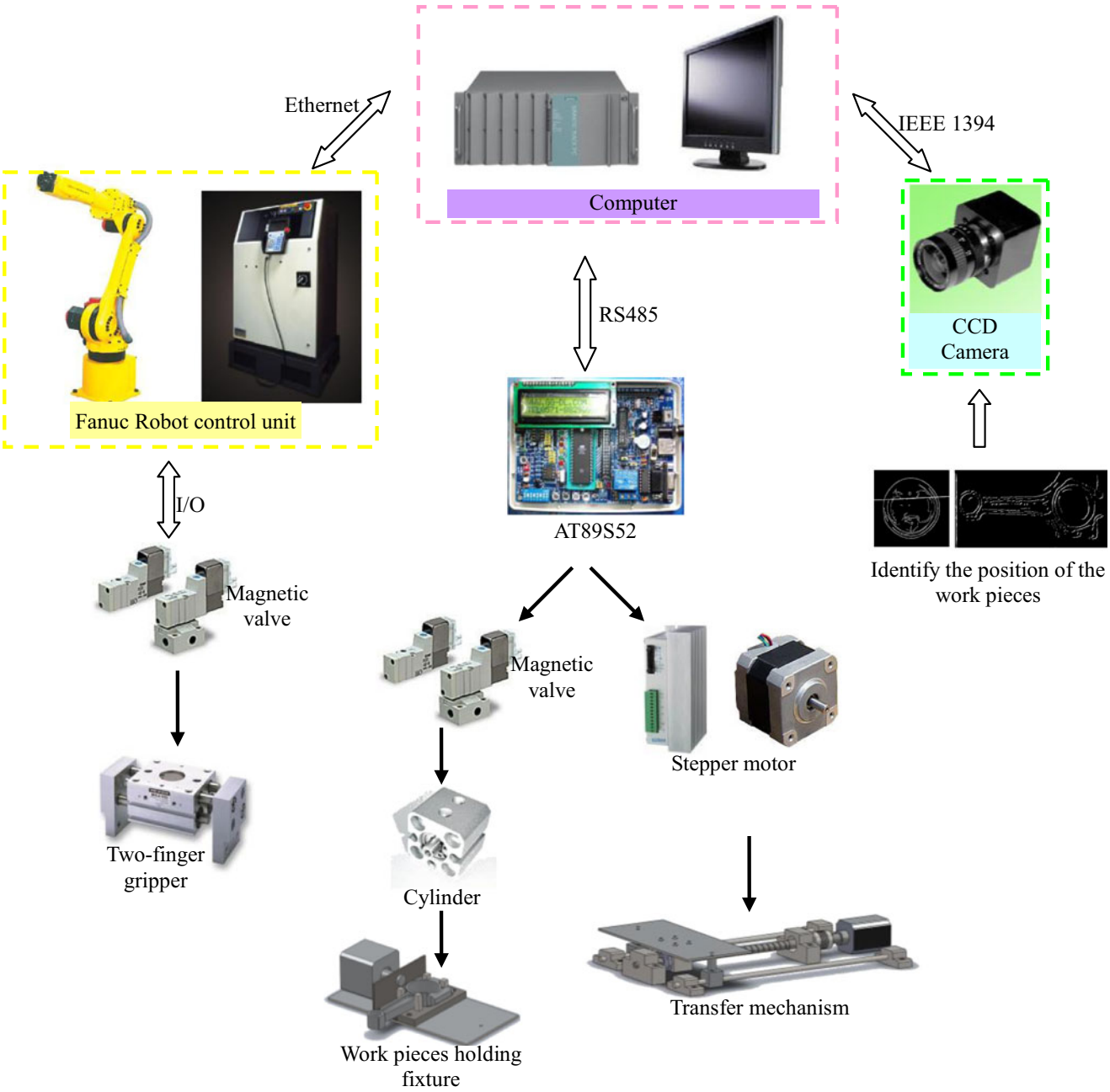

Fig. 2 The structure of the robotic assembly system

transfer the feedback of the fixture and the command of the control computer. The 3D mechanical model and the real fixture are shown in Fig. 3a, b, respectively.

The functions of the fixture are given as follows:

2.3.1 Restrain three translational DoFs and two rotational DoFs of piston by the fixture

As shown in Fig. 3a, the support base is composed of a semi-circular cavity and a locating block, and can prevent the motion of the piston. Two blocks actuated by a bi-directional pneumatic cylinder constrain the rotation of the piston around z-axis and y-axis. One locating block partially prevents the rotation of piston around x-axis. That is, the translation along x, y, and z direction, and the rotation around y- and z-axis (the yaw and pitch rotation except roll rotation) of the piston should be constrained by the fixture.

The translation along x, y, z directions and the roll, pitch, yaw angles of the piston on the fixture's coordinate frame are described in Fig. 4.

As shown in Fig. 5a, the round piston is hard to be totally held by the fixture, i.e., the piston hole has one

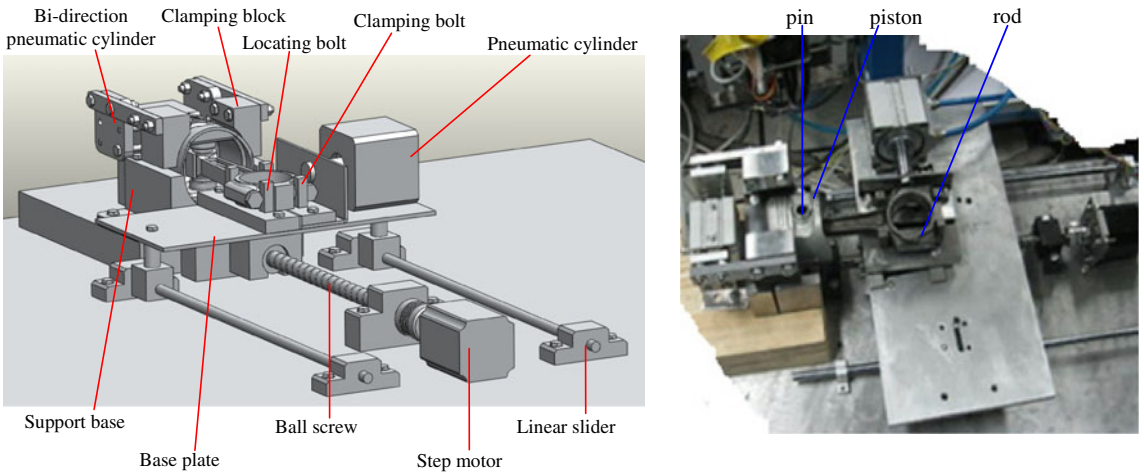

(a) 3D mechanical model of fixture (b) A picture of fixture

Fig. 3 The fixture is designed to hold the rod and piston (**a**) 3D mechanical model of fixture (b) A picture of fixture

degree of freedom unconstrained in the configuration space. Figure 5b is the ideal state for the insertion. It is difficult to design the operations of robot if there is a possible rotation of the hole shown in Fig. 5c or d.

2.3.2 Restrain all motion of the rod by the fixture

It is difficult to decide the position of the four bolts and the initial state of the rod inside the fixture, and it is also hard to ensure the alignment of the hole of the rod and piston. The desired state or undesired state of the rod is determined by the initial state of the rod and the fixture configuration. In Fig. 6a, the clamping bolt is capable to hold the rod to a desired stable state. In Fig. 6b, the rod will arrive to an undesired stable state.

In Section 3, we will discuss the dynamic process of clamping the rod to the expected state, i.e., the rod arrives to the state shown in Fig. 6a.

2.3.3 Transferring the end of rod into the cavity of the piston by the linear guider way

The linear guider way consists of a stepper motor, a ball screw, and two linear sliders. The motion of the linear guide way is controlled by a control board with an AT89S52 single chip. The resolution of positioning of the motion mechanism is decided by the step angle of the stepper motor and the pitch of the ball screw. The linear guider is capable to transfer the rod into the cavity of the piston and keep the piston and rod aligned with the peg.

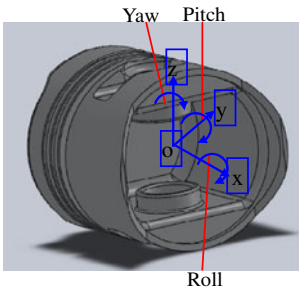

Fig. 4 The coordination frame built on the fixture

3 Clamping strategy of fixture based on attractive region

In this section, we analyze the dynamic process of clamping the rod to the desired stable state based on the conception of attractive region. The desired stable state of the rod is a form closure clamp location and corresponds to the minimum of the attractive region formed by the constraints of the fixture.

3.1 Related conceptions

The conception "attractive region" is briefly introduced below. Assumed that there is a nonlinear system: $dX/dt = f(X, F, t)$, where X is the state of the system, and F is the input to the system. If there is a function $g(X)$, which, for some real number $\varepsilon>0$, satisfies the following properties: for all X in the region $\|X - X_0\| < \varepsilon$ where X_0 is one state of the system:

a) $\begin{cases} g(X) > g(X_0), & X \neq X_0 \\ g(X) = g(X_0), & X = X_0 \end{cases}$;

b) $g(X)$ has continuous partial derivatives with respect to all components of X;

c) $dg(X)/dt < 0$.

Therefore, $\|X\text{-}X_0\|<\varepsilon$ is an attractive region.

The attractive region gives the description of the object's dynamic motion configurations; and therefore, it is suitable

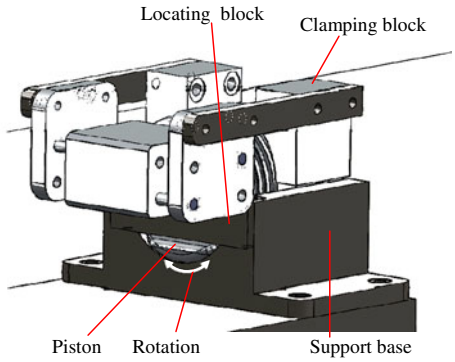

(a) There is a possible rotation around *x*axis

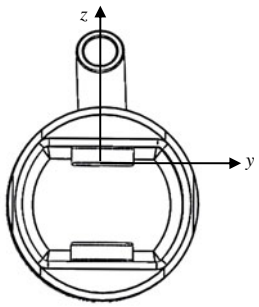

(b) The ideal state of peg-piston for the insertion.

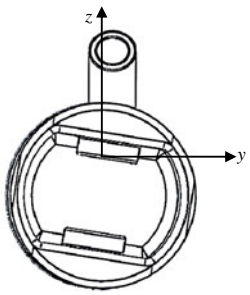

(c) The piston-hole is skewed to the left.

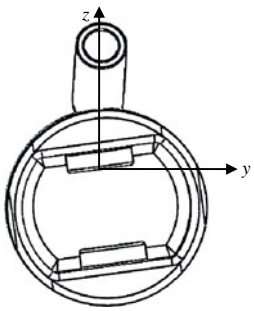

(d) The piston-hole is skewed to the right.

Fig. 5 The state of the piston and the peg. **a** There is a possible rotation around *x* axis **b** The ideal state of peg-piston for the insertion. **c** The piston-hole is skewed to the left. **d** The piston hole is skewed to the right

for the investigation of clamping process. It is defined as a set of object configurations from which the object could be pulled to the desired stable state under the pre-specified input.

Form closure, which is related to the ability of preventing all the motion of clamped object, should be guaranteed for restraining objects [22–24].

In this section, the dynamic processing to keep the rod at the desired state is discussed based on the attractive region. And the relationship between the local minimum of the attractive region and the form-closure clamping is described briefly.

3.2 Clamping the rod to the desired stable state

A reference coordinate established on the fixture is shown in Fig. 7: *xoy* is the fixture coordinate, and *O* is the origin of the clamping coordinate, O_c is the center of the big end of the rod.

Initially, the origin *O* of the frame is at the center of the fixture. The tuple (x_o,θ) is used to describe the rod pose, where x_0 is the *x*-coordinate of O_c, and θ denotes the rotation angle between OO_c and *x*-axis.

The edges of the rod which would be contacted by the bolts of fixture are denoted by the line equation:

$$E_k(a_k, b_k) = 0,\ k = 1, 2, 3, 4$$

where a_k is the slope, b_k is the intercept of the line E_k.

p_1,p_2 (solid points in the Fig. 7) are the intersection points of c_1c_4 and the rod, and p_3,p_4 are the intersection points of c_2c_3 and the rod. Thus, the distance *D* between the clamping bolts and locating bolts can be formulated as:

$$\begin{aligned} &D = 2 \cdot \max\{|y_1|, |y_2|, |y_3|, |y_4|\} \\ &\text{s.t. } E_1\left(-\frac{r}{2}, y_1\right) = 0,\ E_2\left(-\frac{r}{2}, y_2\right) = 0 \\ &E_3\left(\frac{r}{2}, y_3\right) = 0,\ E_4\left(\frac{r}{2}, y_4\right) = 0 \end{aligned}$$

Where y_1 is *y* coordinate of the point p_1, y_2 is for p_2, y_3 is for p_3 and y_4 is for p_4, *r* is the distance of the c_3 and c_4.

y_i (i=1,2,3,4) is determined by the rod pose, which can be described by the tuple (x_0, θ). Therefore, the attractive region formed by the constraints of the four bolts in the configuration space can be described by the distance *D* and the tuple (x_0, θ). Figure 8 shows the simulation of attractive region. Some bowl-like figures are formed in the configuration space. Each point on the curve indicates a pose of the rod. The minimum point D_0 of the figure represents the desired stable state of the rod.

In Fig. 8, D_1 and D_0 are the values of distance *D* at state X_1 and state X_0, respectively. The side length of the big end of the rod is 50 mm, the distance between the bolt c_1 and bolt c_2 is 60 mm. The simulation region is $x_0 \in$ (−29.7, 29.7 mm), $\theta \in (-\pi/4, \pi/4)$.

The attractive region which ensures the rod being converged to the desired state is shown in Fig. 8. If the

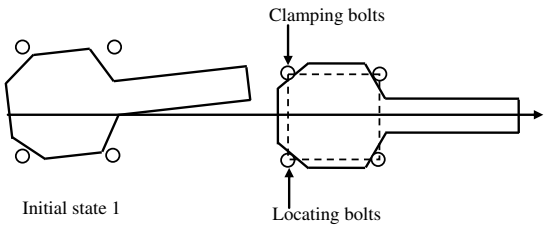

(a) The rod arrives to the desired state from initial state 1 under the clamping force of the bolts.

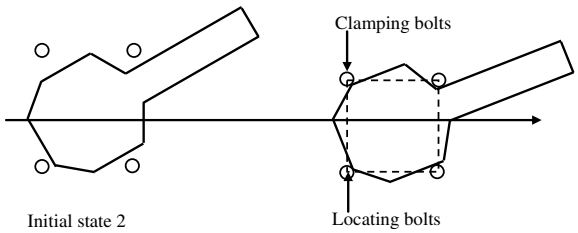

(b) The rod arrives to an undesired state from the initial state 2 under the clamping force of the bolts.

Fig. 6 Clamping the rod to a desired state. **a** The rod arrives to the desired state from *initial state 1* under the clamping force of the bolts. **b** The rod arrives to an undesired state from the *initial state 2* under the clamping force of the bolts

state of the rod is at the initial state inside the attractive region, e.g., state X_1, it should be transferred to the stable state X_0 under the squeeze force of the four bolts. At the stable state X_0, the position uncertainties of the rod should be eliminated by the constraints of the four bolts c_i (i=1,2,3,4). In other words, the local minimum of the bowl-like attractive region corresponds to a form closure clamping. The desired stable state of rod indicates that the center of the rod coincides with the origin of the fixture and the center line of the rod aligns to the x-axis.

As the attractive region in the configuration space is built, the manipulations to make the rod to the desired stable state are:

1. Place the rod with some initial states in the attractive region.
2. Squeeze the rod by the two clamping bolts.

Thus, the rod would be transferred from the initial state to the desired stable state. After the rod is fixed on the fixture, the next operation is to insert the peg into the hole, as discussed in the next section.

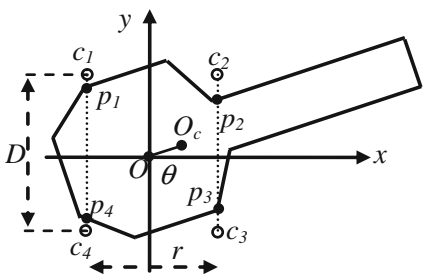

Fig. 7 The reference establishment for clamping the rod, where c_1 and c_2 (*hollow points*) are the clamping bolts, c_3 and c_4 are the locating bolts of the fixture

4 Peg-in-hole insertion strategy based on attractive region

In our previous work [1, 25], a sensorless peg-in-hole insertion strategy was discussed based on attractive region, where the hole was supposed to be fully constrained to a known state. In the previous work, attractive region was used to eliminate the uncertainty of the peg state with the aid of constraints from the hole. However, in the peg–piston–rod assembly, the orientation uncertainty of the piston hole is difficult to be totally eliminated by the fixture. The unconstrained DOFs of hole will make it difficult to apply the available strategies. In order to complete the peg-in-unfixed-hole insertion successfully, a new approach is proposed in the following. The strategy takes the pose uncertainty caused by relative motion of the peg and the piston hole into consideration.

4.1 The attractive region formed in the configuration space of the peg-hole system

In this subsection, the attractive region formed in the configuration space of the peg-hole system is proposed firstly. And then, it is used to analyze the characteristics of contact states between the peg and the hole.

Denoted by X_p and X_h the states of the peg and the hole in the world's coordinate, which can be represented with six degrees of freedom: *x, y, z,* pitch, roll, and yaw, as described below.

$$X_p = \left[x_p, y_p, z_p, \theta_{px}, \theta_{py}, \theta_{pz}\right]$$

$$X_h = \left[x_h, y_h, z_h, \varphi_{hx}, \varphi_{hy}, \varphi_{hz}\right]$$

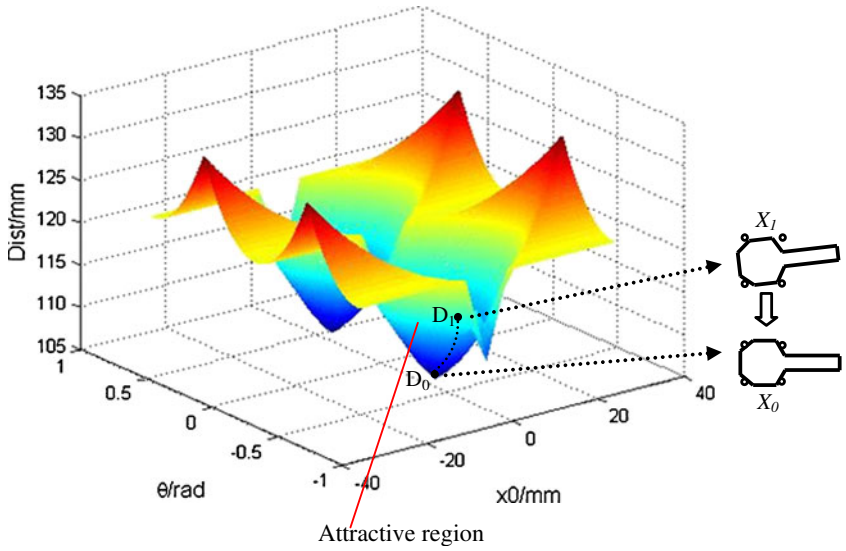

Fig. 8 Simulations of motion region of the rod in the configuration space

As shown in Fig. 9, there are three coordinate frames used in the analysis of the assembly process:

1. A world's coordinate, i.e., *xyz*-coordinate, is built on the base of the fixture.
2. H coordinate frame is fixed with the hole, where O_h is defined as the center of the upper surface of the hole, and O_hY_h is defined as the line from O_h to the base of the fixture, O_hZ_h is along the axis of the hole upwards and O_hX_h is perpendicular to O_hY_h and O_hZ_h.
3. P coordinate frame is fixed with the peg, where O_p is defined as the center of the end surface of the peg, O_pY_p is parallel to the projection of the O_hY_h on the end surface of the peg, O_pZ_p is along the axis of the peg upwards and O_pX_p is perpendicular to O_pZ_p and O_pX_p.

In general, the location of the peg in the world's coordinate frame can be described by $\left(x_h, y_h, z_h, \varphi_{hx}, \varphi_{hy}, \varphi_{hz}\right)$, and the location of the hole in the world's coordinate frame can be defined by $\left(x_p, y_p, z_p, \theta_{px}, \theta_{py}, \theta_{pz}\right)$. In the assembly process, five DOF of the hole are constrained by the fixture, i.e., $(x_h, y_h, z_h, \varphi_{hy}, \varphi_{hz})$ should keep their initial value when the piston is clamped by the fixture. Suppose the state of the peg-hole system is denoted by X_{ph} in the world's frame, one can obtain:

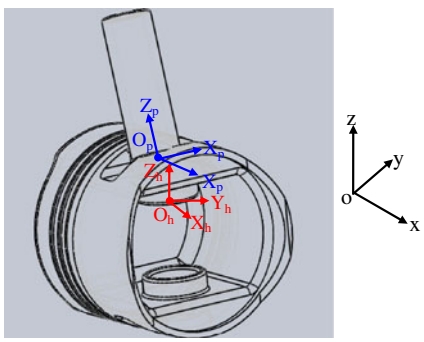

Fig. 9 The coordinate frames built on the peg and the hole

$$X_{ph} = \left(x_p, y_p, z_p, \theta_{px}, \theta_{py}, \theta_{pz}, \varphi_{hx}\right)$$

The rotation of peg around *x*-axis and *y*-axis, i.e., angle θ_{px} and θ_{py}, are decided by the translation and rotation of peg relative to piston hole. Thus, the motion of the peg-hole system in the world's coordinate frame can be described by the relative pose of the peg in the H coordinate frame. The pose of peg is defined as below:

$$X = \left(x_{ph}, y_{ph}, z_{ph}, \phi_{phx}, \phi_{phy}, \theta_{pz}\right)$$

where x_{ph}, y_{ph}, z_{ph} represent the translation of peg on the H-coordinate frame. ϕ_{phx}, ϕ_{phy} represent the rotation of peg around O_hX_h axis and O_hY_h axis, θ_{px} represents the rotation of peg around *z*-axis.

The rotation around *z*-axis of the axially symmetric peg cannot change the distance between O_p and O_h, so, θ_{px} would be ignored in the next discussion. We can construct an attractive function as follows:

$$z = g(X_s) = g\left(x_{ph}, y_{ph}, \phi_{phx}, \phi_{phy}\right)$$

where $z=z_{ph}$ is the distance between O_p and O_h.Therefore, (X_s, z)construct the configuration space of peg-hole system.

The state of the peg-hole system can be divided into a translational vector and a rotational vector.

$$X_s = [X, Y]$$

where $X = (x, y) = (x_{ph}, y_{ph}), Y = (\phi_r, \phi_m) = (\phi_{phx}, \phi_{phy})$.

In our former work [25], the peg-in-hole strategy is explored in the configuration space constructed by (*X, z*), where *X* is the translation along *x* and *y* directions of peg. The contact states of peg hole and the points on the attractive region formed in the three-dimensional configuration space are shown in Fig. 10. Each point inside the region but on the boundary corresponds to one peg-hole configuration without contact points between the peg and the hole. Each point on the boundary corresponds to one peg-hole contact state.

In this paper, the peg-in-hole strategy is designed in configuration space constructed by $z = g(X, Y)$, where (*X, Y*) defines the translation and rotation of peg-hole system. In the following, we discuss a method to decompose the high-dimensional configuration space into two low-dimensional configuration spaces. The aim is to have insight on system analysis and achieve easy design of the insertion strategy in the two sub-configuration spaces.

4.2 The decomposition of the attractive function

In this subsection, a map $t: Y \rightarrow X$ provided by the function $z = g(X, Y)$ is discussed, so that the configuration space of the system can be divided into two sub-configuration spaces corresponding to the mapping function, as illustrated in the following.

We assume that $g: X \times Y \rightarrow z$ defines a smooth hypersurface in the configuration space. For every point on this hypersurface, there is infinite number of tangent lines. The partial differentiation of this hypersurface will allow choosing one of these lines and finding its slope. To find the slope of the line tangent to the function at a point that is parallel to the *zX* hyperspace, the *Y* variable is treated as constant. And, the minimum and maximum of the function when the *Y* variable is treated as constant can only occur at the point where the slope equals to zero [26], as given in Eq. 1:

$$D_X g(X, Y) = 0 \tag{1}$$

where D_x is the first partial derivative with respect to *X*.

In the following, based on the partial differentiation of attractive function in the Eq. 1, we discuss the method to decompose the configuration space by mapping *Y* to *X*.

a. A map $t: Y \rightarrow X$ is performed as follows:

Set $Y = Y^*$, where Y^* is treated as constant. Suppose the minimum of $g(X, Y^*)$ is denoted by $g(X^*, Y^*)$, as given in Eq. 2

$$g\left(X^*, Y^*\right) = \min_X g\left(X, Y^*\right) \tag{2}$$

Assume that $D_{XX} g\left(X, Y^*\right) > 0$, where D_{xx} is the second-order partial derivative with respect to *X*. Thus, solution to the minimum of function $g\left(X, Y^*\right)$, X^* can be computed from Eq. 3:

$$D_X g\left(X, Y^*\right) = 0 \tag{3}$$

If $D_X g\left(X, Y^*\right)$ is continuous, then there exists an open set *U* containing X^*, an open set *V* containing Y^*, and a differentiable function:

$$t : Y^* \rightarrow X^*$$

Therefore, Eq. 2 can be expressed by:

$$g\left(t(Y^*), Y^*\right) = \min_X g\left(X, Y^*\right) \tag{4}$$

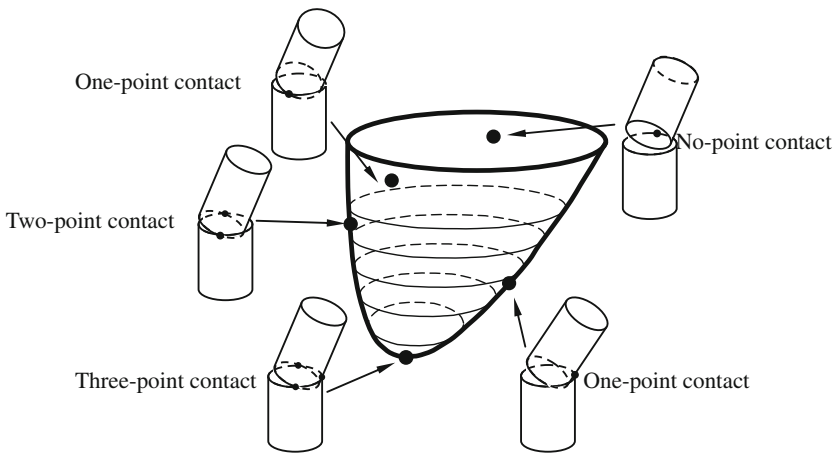

Fig. 10 The relationship between the points on the attractive region and the contact states of the peg hole

In the following, the method to decompose graph $(z, X, Y)$to two subgraphs $(z, X)$and $(z, Y)$is proposed based on the discussion of the implicit function $t : Y \to X$.

(b) The decomposition of graph$(z, X, Y)$is performed as follows:

Suppose $Y^* + \Delta Y$ be a vector in the neighborhood of Y^*, one can obtain

$$g\left(t\left(Y^* + \Delta Y\right), Y^* + \Delta Y\right) = \min_X g\left(X, Y^* + \Delta Y\right)$$

$z = g(X, Y)$is a continuous function, thus:

$$\min_X g\left(X, Y^*\right) = \lim_{\Delta Y \to 0}\left(\min_X g\left(X, Y^* + \Delta Y\right)\right)$$

Thus,

$$g\left(t(Y^*), Y^*\right) = \lim_{\Delta Y \to 0} g\left(t(Y^* + \Delta Y), Y^* + \Delta Y\right)$$

That is, $z = g\left(t(Y^*), Y^*\right)$ is continuous in the hyperspace.

Thus, the minimum of $z = g(X, Y)$ can be obtained by the following two steps:

For a $Y_i \in U$, we assume that:

$$z_i = g(t(Y_i), Y_i)$$

And then, we can obtain the minimum z_0 of z_i as follows:

$$z_0 = \min_i z_i$$

Then, the two attractive functions can be visualized in the sub-configuration space. The process of convergence to the minimum of the two attractive functions can be realized in the following two stages.

4.2.1 The attractive region formed in the sub-configuration space of peg-piston system with a fixed orientation

We assume that the orientation of the peg is fixed, i.e., two rotational angles $Y = (\phi_r, \phi_m)$ are kept unchanged. Thus, the motion of the peg-piston system can be described by two variables $(O_pO_h)_x$(the translation along x-axis) and $(O_pO_h)_y$ (the translation along y-axis), which are the movements of the center O_p of peg related to the center $O_h$of the hole.

The attractive function formed in the sub-configuration space, as $(\phi_r, \phi_m) = (-\alpha, 0)$, is established as follows:

$$(O_hO_p)_z = \frac{\sqrt{\left(R_h - R_p\cos\alpha\right)^2 + \sin\alpha\left(R_h^2 - R_p^2\right)}}{\sin\alpha}(1 - \cos\alpha)$$

$$(O_hO_p)_y \in [-R_h, R_h]$$

$$(O_hO_p)_x \in [-R_h(1 + \cos\alpha), R_h(1 - \cos\alpha)]$$

where $R_h$and R_p are the radii of the peg and hole, respectively.

The graph of the attractive function in the configuration space with fixed orientation is presented in Fig. 11.

In Fig. 11, the attractive region is used to eliminate the translation uncertainties of the peg with respect to the hole. When $(O_pO_h)_z$(the translation along z-axis) is not changeable, the attractive function has a local minimum at the fixed orientation $Y = (-\alpha, 0)$, where the translation of the peg is restrained by the hole.

4.2.2 The attractive region formed in sub-configuration space of peg–piston system with orientation changes

We assume that the orientation of the peg–piston changes with $Y_n, ..., Y_1, Y_0$. And, at each orientation $Y_i (i = 1, 2, ..., n)$, the process to obtain the minimum of the attractive function is discussed in the previous section (Section 4.2.1). At the local minimum of the attractive region, the translation $X_i = (x_i, y_i)$ is determined by the rotation $Y_i = (\phi_{ri}, \phi_{mi})$ from the mapping function $t : Y \to X$. That is, the movement region of peg-hole system is decided by the rotation angles.

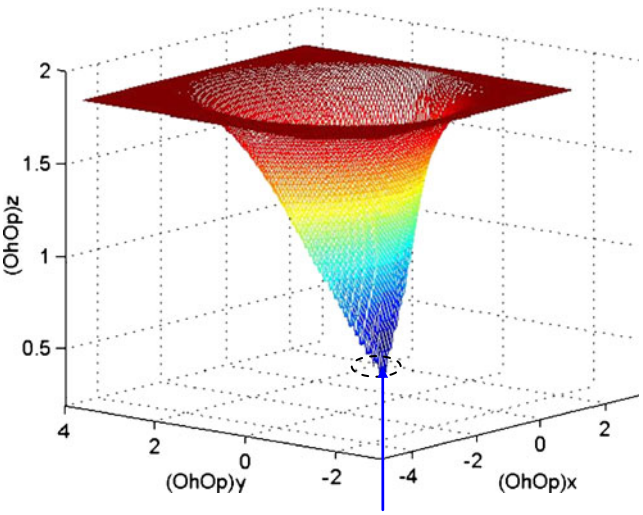

Fig. 11 The graph of the attractive function with fixed orientation, the minimum of the graph represents a three-point contact state of the peg hole

The attractive function of the peg-hole with orientation changes is established as follows:

$$z = \frac{\sqrt{\left(R_{\mathrm{h}} - R_{\mathrm{p}}\cos\phi_{\mathrm{r}}\cos\phi_{\mathrm{m}}\right)^2 - \sqrt{\left(1-\cos^2\phi_{\mathrm{r}}\cos^2\phi_{\mathrm{m}}\right)}\left(R_{\mathrm{h}}{}^2 - R_{\mathrm{p}}{}^2\right)}}{\sqrt{1-\cos^2\phi_{\mathrm{r}}\cos^2\phi_{\mathrm{m}}}}\left(1-\cos\phi_{\mathrm{r}}\cos\phi_{\mathrm{m}}\right)$$

$$y \in [-R_{\mathrm{h}}, R_{\mathrm{h}}]$$

$$x \in [-R_{\mathrm{h}}(1+\cos\phi_{\mathrm{r}}\cos\phi_{\mathrm{m}}), R_{\mathrm{h}}(1-\cos\phi_{\mathrm{r}}\cos\phi_{\mathrm{m}})]$$

where R_{h} and R_{p} are the radius of the peg and hole, respectively.

The graph of the attractive function in the configuration space is presented in Fig. 12.

When the attractive function achieves the minimum, the orientation and position of the peg–piston system are determined by the following equation.

$$z_0 = \min_i z_i$$

where z_0 is the minimum of the attractive function $z = g(X, Y)$, which corresponds to the case that the peg has been inserted into the hole of piston.

Therefore, as illustrated in Sections 4.2.1 and 4.2.2, the peg-in-piston insertion process is divided into two steps:

Step 1 For a fixed orientation of the peg–piston system, design a nominal input which enables the peg–piston system to follow a nominal trajectory to reach to the local minimum of the attractive region, where the translation uncertainties of the peg can be eliminated by the constraints of the hole.

Step 2 When the orientation changes, design an adjustable input which attracts the peg–piston system to the minimum of the attractive region, where the rotation uncertainties of the peg–piston can be eliminated by the constraints of the fixture.

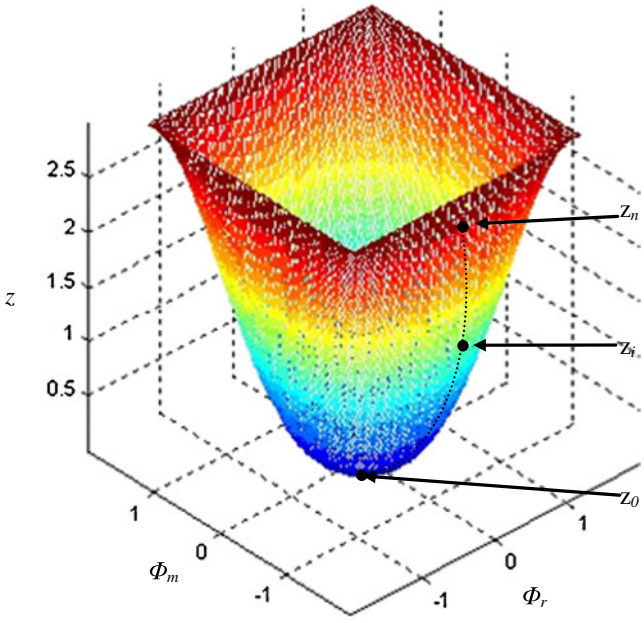

Fig. 12 The attractive region of the peg-hole system with orientation changes

Therefore, the state of the peg hole should be in compliance to the path shown in Fig. 12. At the minimum of the graph, position and orientation uncertainties between the peg and hole are eliminated by the constraints of the hole. In the following, the experiment illustrates the validity of the proposed strategy.

4.2.3 Realizing the insertion operation with the compliance of the robot

The explanations of the attractive region and the practical manipulations of the robot are introduced in Fig. 13. "Soft float", which allows the robot path to be changed according to the external force to achieve the desired result, can be used to act as the adjustable input. The function of "soft float" of M6i-B can be set on the controller. Guided by the vision, the peg held by a two-finger gripper can be moved from any initial position into the mouth of the hole. And then, in Cartesian mode, we can control the robot to:

Stage 1 Adjust the peg to let $Y_{\mathrm{i}} = (\phi_{\mathrm{ri}}, \phi_{\mathrm{mi}})$, then

a. The translational DOFs of the robot along the x-axis and z-axis are configured by "soft float", the peg moves along y-axis as a result of an applied force. Stop the motion of the peg when the translation along y-axis, i.e., $(O_{\mathrm{h}}O_{\mathrm{p}})_y$, is not changed.
b. The translational DOFs of the robot along the y-axis and z-axis are configured by "soft float", the peg moves along x-axis with a force and stopped by the hole when $(O_{\mathrm{h}}O_{\mathrm{p}})_x$ is not changed.
c. The peg moves along $-z$-axis with a force, and stopped by the hole when $(O_{\mathrm{h}}O_{\mathrm{p}})_z$ is not changed.

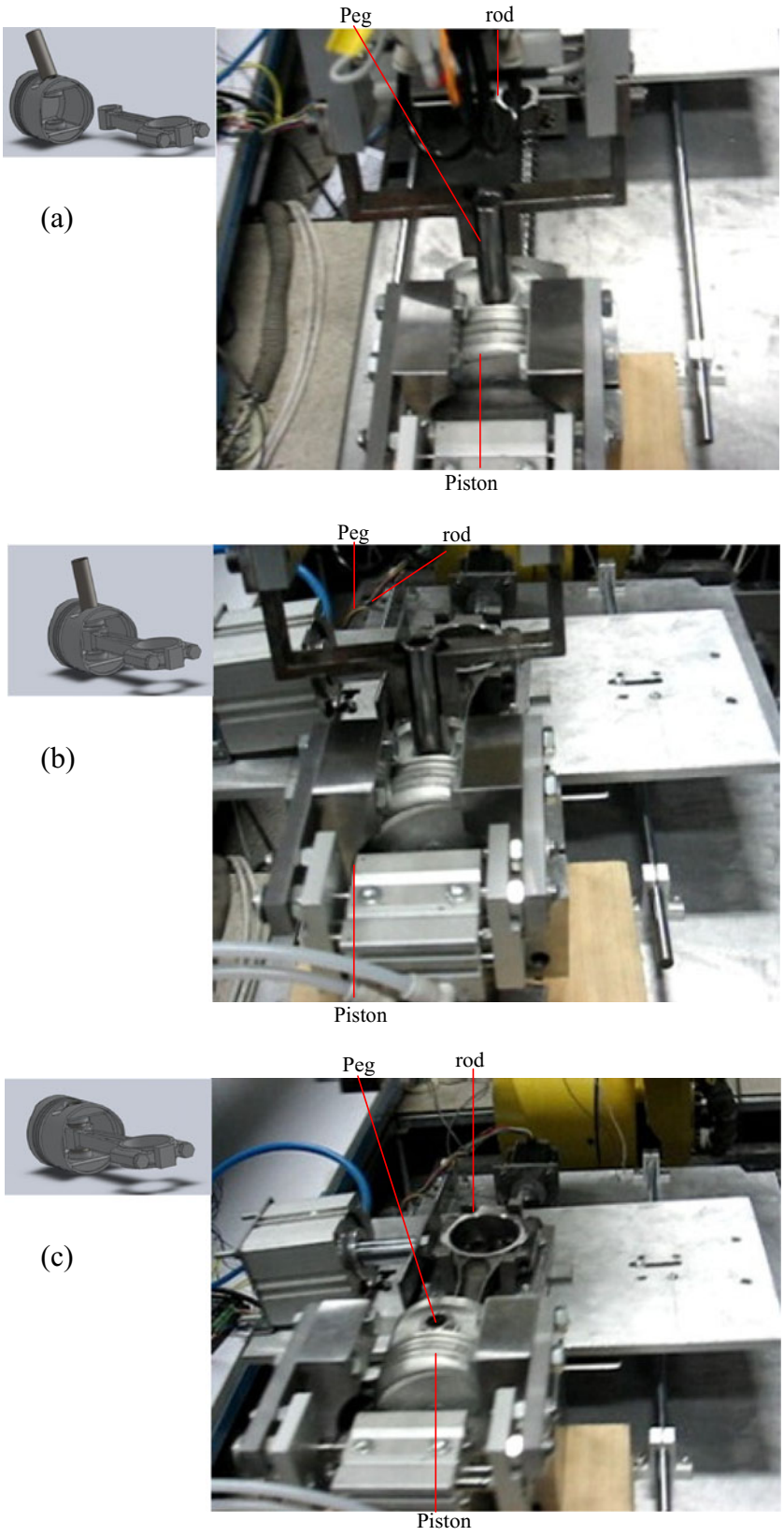

Fig. 13 The assembly process of the peg and piston. **a** Guided by the visual information, the peg held by a two-finger gripper with fixed angle can be moved from any initial position into the mouth of the hole. **b** The peg rotates around x, y, and z-axis with a small angle, i.e., the orientation of the peg changes from Y_i to Y_{i-1}. **c** When the rotation and the translation of the peg (x, y, ϕ_r, ϕ_m) is not changeable, which means that the peg has been inserted into the hole

Explanation 1 The peg moves along x, y and z-axis with a fixed orientation $Y_{\mathrm{i}} = (\phi_{\mathrm{ri}}, \phi_{\mathrm{mi}})$ and stopped by the hole when the translation of the peg is not change. That is, for a fixed orientation of the peg-hole system, the attractive

function should achieve the local minimum at the state $(t(Y_i), Y_i)$.

$$z_i = g(t(Y_i), Y_i)$$

At the local minimum of the attractive region, the translation uncertainties of the peg should be eliminated, i.e., the x, y, z position of the peg is decided. The next step is to eliminate the uncertainties of two related variables ϕ_r and ϕ_m.

Stage 2 Adjust the peg to let $Y_i$to $Y_{i-1}, ..., Y_0$

a. The rotational DOFs of the robot around x-axis and z-axis are configured by "soft float", and the peg rotates around y axis with a small angle $\Delta\phi_{\mathrm{mi}}$, i.e., the orientation of the peg changes from $Y_i = (\phi_{\mathrm{ri}}, \phi_{\mathrm{mi}})$ to $Y_{\mathrm{i}-1} = (\phi_{\mathrm{ri}}, \phi_{\mathrm{mi}} - \Delta\phi_{\mathrm{mi}})$. Then, at the fixed orientation $Y_{\mathrm{i}-1}$, the peg moves to the local minimum $g(t(Y_{i-1}), Y_{i-1})$, which is similar to the stage 1.
b. The rotational DOFs of the robot around the y-axis and z-axis are configured by "soft float", and then the peg rotates around x-axis by a small angle $\Delta\phi_{\mathrm{ri}}$, i.e., the orientation of the peg changes from $Y_{\mathrm{i}-1} = (\phi_{\mathrm{ri}}, \phi_{\mathrm{mi}} - \Delta\phi_{\mathrm{mi}})$ to $Y'_{i-1} = (\phi_{\mathrm{ri}} - \Delta\phi_{\mathrm{ri}}, \phi_{\mathrm{mi}} - \Delta\phi_{\mathrm{mi}})$. Then, at the fixed orientation Y'_{i-1}, the peg moves to the local minimum $g\left(t(Y'_{i-1}), Y'_{i-1}\right)$, which similar to the stage 1.
c. Stop the rotate when $(\mathrm{O_hO_p})_z$ is not changeable, which means that the peg has been inserted into the hole.

Explanation 2 The inserting force is designed to change the state of the Y_i to $Y_{i-1}, ..., Y_0$ in the attractive region, thus the minimum of $z = g(X, Y)$ converge to $z_0 = g(t(Y_0), Y_0)$ as the Y_i approaches to Y_0, where $z_0 = g(t(Y_0), Y_0)$is the minimum value of $z_i = g(t(Y_i), Y_i)$, that is

$$\begin{aligned} z_0 &= g(t(Y_0), Y_0) \\ &= \min_i g(t(Y_i), Y_i) \end{aligned}$$

As shown in Fig. 13a, guided by the visual information, the peg held by a two-finger gripper with fixed angle can be moved from any initial position into the mouth of the hole. The rotational DOFs of the robot around x-axis and z-axis are configured by "soft float", that is, the angles between the axis of the peg and the hole around x-axis and z-axis may remain free of control and can be also eliminated during the rotating process, as shown in Fig. 13b; and the peg is inserted into the hole of piston finally, as shown in Fig. 13c.

Then, at the fixed orientation Y_{i-1}, the peg moves to the local minima $z_{i-1} = g(t(Y_{i-1}), Y_{i-1})$.

In the following, the whole assembly process of peg into hole of piston and rod is described.

5 The assembly process

In the former section, based on the concept of "attractive region", we discussed the strategy of insertion of a peg into a hole of a piston. The real assembly workcell built in the lab is shown in the Fig. 14.

In Fig. 15, the manipulations of the robot, such as identifying, grasping, and inserting, are described in briefly by a flowchart. With the aid of visual information, a target piston at an arbitrary place should be identified from a set of parts, and then the two-finger gripper should be guided to pick and place a target to the fixture.

6 Conclusion

In this paper, we propose a new sensorless manipulation strategy for inserting a peg into an unfixed hole based on the attractive region formed by contact constraints. The approach aims to propose the robotic manipulations in the subspaces of the high-dimensional configuration space of peg-hole system, which ensures robotic motion planning, could be visualized in the low-dimensional space. Moreover, based on the analysis about the attractive region, the manipulations to make the rod to be clamped in the desired stable state are described.

Usually, the sensorless peg-in-hole strategy is explored in the configuration space (X, z), where X is the translation along x and y direction of peg. However, for the insertion of a peg into an unfixed hole, the motion planning should be designed in configuration space (X, Y, z), where (X, Y) is the translation and rotation of both the peg and the hole. In this paper, a map $t : Y \to X$ provided by the function $z = g(X, Y)$ is established to divide the high-dimensional

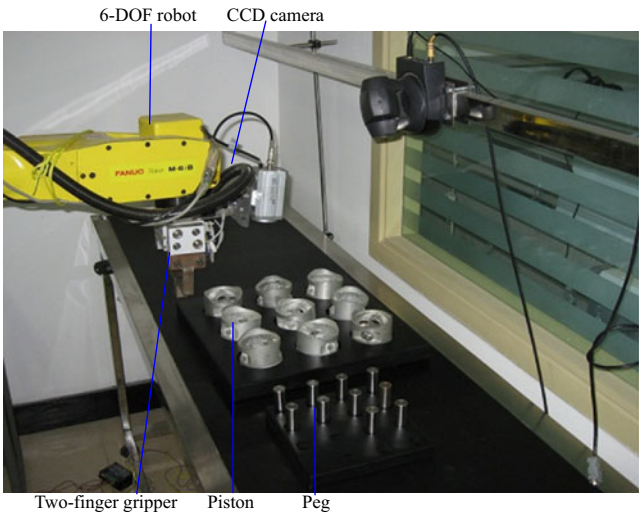

Fig. 14 The overview of the robotic assembly system

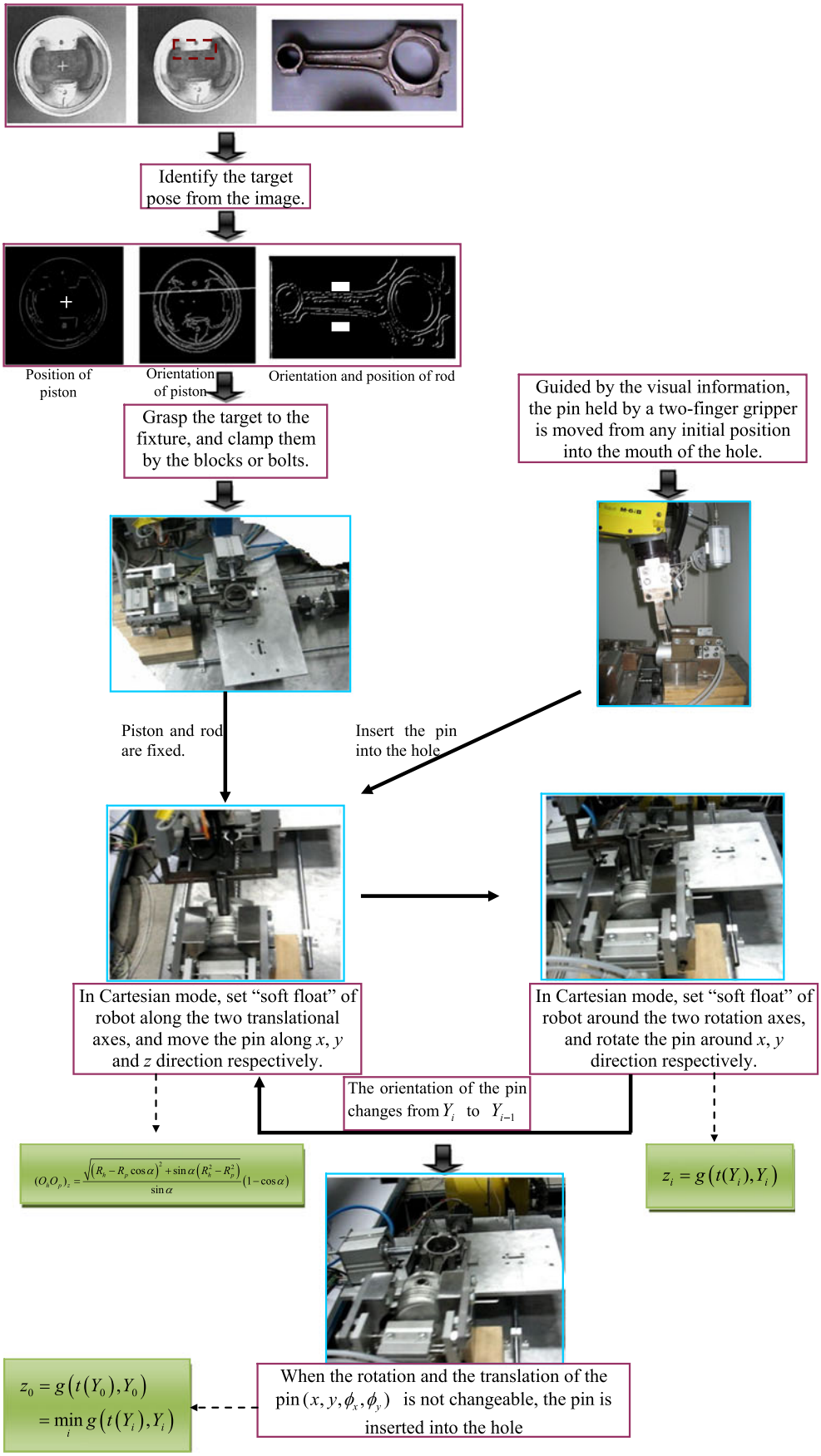

Fig. 15 The flowchart of the whole assembly process

configuration space into two subspaces (z, X) and (z, Y). With the aid of the attractive regions formed in the two subspaces, the position and orientation uncertainties of the peg hole are eliminated by the designed robotic manipulations.

Finally, the methods are validated by the simulations and experiments of the assembly of the piston, peg, and rod of the automotive engine on the built robotic system.

Acknowledgments The authors would like to thank Yuren Zhang, Yongkang Luo for their help on the simulations and figures of the manuscript. The authors would also like to thank Minyu Fan and Junaid Khan for his constructive suggestions, which improved the readability of this paper.

References

1. Qiao H (2002) Strategy investigation with generalized attractive regions. IEEE Int. Conf. on Robotics and Automation pp 3315–3320
2. Inoue H (1974) Force feedback in precise assembly tasks. AIM 308 Artificial Intelligence Lab MIT
3. Whitney DE (1982) Quasi-static assembly of compliantly supported rigid parts. Trans. ASME J. Dynamic Systems. Measurement and Control 104(1):65–77
4. Loiano-Perer T, Winston PH (1987) LAMA: a language for automatic mechanical assembly. 5th. Int. Joint. Conf. Artificial Intelligence pp 710–716
5. Schutter JD, Katupitiya J, Vanherck P, Brussel HK (1987) Active force feedback in industrial robotic assembly: a case study. Int J Adv Manuf Technol 2:27–40. doi:10.1007/BF02601491
6. Katz Z, van Wyk RSJ (1997) Analysis of peg-hole automated pre-assembly engagement search. Int J Adv Manuf Technol 13:426–433. doi:10.1007/BF01179038
7. Yao YL, Cheng WY (1999) Model-based motion planning for robotic assembly of non-cylindrical parts. Int J Adv Manuf Technol 15:683–691. doi:10.1007/s001700050119
8. Zhang WJ, Mao TX, Yang RQ (2005) A new robotic assembly modeling and trajectory planning method using synchronized Petri nets. Int J Adv Manuf Technol 26(4):420–426. doi:10.1007/s00170-003-1995-1
9. Tangjitsitcharoen S, Rojanarowan N, Tangpornprasert P, Virulsri C (2009) Intelligent control of microassembly process based on in-process monitoring of pressing force. Int J Adv Manuf Technol 45:148–155. doi:10.1007/s00170-009-1946-6
10. Shirinzadeh BJ, Zhong YM, Tilakaratna PDW, Tian YL, Dalvand MM (2010) A hybrid contact state analysis methodology for robotic-based adjustment of cylindrical pair. Int J Adv Manuf Technol 52(4):329–342. doi:10.1007/s00170-010-2705-4
11. Whitney DE, Rourke JM (1986) Measurement and C mechanical behavior and design equations for elastomer shear pad remote center compliances. ASME J Dynamic Systems Control 108:223–232
12. Simunovic S (1975) Force information in assembly processes. Proc. 5th Int. Symp. on Industrial Robots pp 415–431
13. Asada H, Kakumoto Y (1988) The dynamic RCC hand for high-speed assembly. IEEE Int. Conf. on Robotics and Automation pp 120–125
14. Ivanov RV (1989) Scanning assembly. Int J Adv Manuf Technol 4:95–102
15. Lee S (2005) Development of a new variable remote center compliance with modified elastomer shear pad for robot assembly IEEE Trans. on Automation Science and. Engineering 2:193–197
16. Siciliano B, Khatib O (2008) Springer handbook of robotics. Springer-Verlag Berlin and Heidelberg
17. Matsuno T, Fukuda T, Hasegawa Y (2004) Insertion of long peg into tandem shallow hole using search trajectory generation without force feedback. IEEE Int. Conf. on Robotics and Automation pp 1123–1128
18. Caine ME, Lozano-Perez T and Seering WP (1989) Assembly strategies for chamferless parts. IEEE Int. Conf. Robotics and Automation pp 472–477
19. Chen HP, Wang JJ, Zhang G, Fuhlbrigge T, Kock S (2009) High-precision assembly automation based on robot compliance. Int J Adv Manuf Technol 45:999–1006. doi:10.1007/s00170-009-2041-8
20. Balkcom DJ, Gottlieb EJ, Trinkle JC (2002) A sensorless insertion strategy for rigid planar parts. IEEE Int. Conf. on Robotics and Automation pp 882–887
21. Ji X, Xiao J (2001) Planning motion compliant to complex contact states. Int J of Robotics Research 20(6):446–465
22. Bicchi A (1995) On the closure properties of robotic grasping. Int J Robot Res 14(4):319–334
23. Brost RC, Goldberg KY (1996) A complete algorithm for designing planar fixtures using modular components. IEEE Trans on Robotics and Automation 12(1):31–46
24. Nguyen VD (1986) Constructing force-closure grasps. IEEE Int Conf Robot Autom 3:1368–1373
25. Qiao H and Tso SK (1999) A new space used in sensor-less manipulation. IEEE/RSJ Int. Conf. on Intelligent Robots and Systems pp 924–929
26. Kudryavtsev LD (2001) Implicit function. Hazewinkel, michiel, encyclopedia of mathematics. Springer, ISBN 978–1556080104